# Generalization in Quantum Machine Learning: a Quantum Information Perspective

Leonardo Banchi,[1,2,*] Jason Pereira,[3,1] and Stefano Pirandola[3]

[1]*Department of Physics and Astronomy, University of Florence,*
*via G. Sansone 1, I-50019 Sesto Fiorentino (FI), Italy*
[2]*INFN Sezione di Firenze, via G. Sansone 1, I-50019, Sesto Fiorentino (FI), Italy*
[3]*Department of Computer Science, University of York, York YO10 5GH, UK*

We study the machine learning problem of generalization when quantum operations are used to classify either classical data or quantum channels, where in both cases the task is to learn from data how to assign a certain class $c$ to inputs $x$ via measurements on a quantum state $\rho(x)$. A trained quantum model generalizes when it is able to predict the correct class for previously unseen data. We show that the accuracy and generalization capability of quantum classifiers depend on the (Rényi) mutual informations $I(C{:}Q)$ and $I_2(X{:}Q)$ between the quantum embedding $Q$ and the classical input space $X$ or class space $C$. Based on the above characterization, we then show how different properties of $Q$ affect classification accuracy and generalization, such as the dimension of the Hilbert space, the amount of noise, and the amount of neglected information via, e.g., pooling layers. Moreover, we introduce a quantum version of the Information Bottleneck principle that allows us to explore the various tradeoffs between accuracy and generalization.

## I. INTRODUCTION

Quantum information and machine learning are two very active areas of research which have become increasingly interconnected [1–4]. In this panorama, many works have considered and designed learning models that are built by using quantum states and algorithms [5–15]. Some of these proposals have focused on learning classical data by exploiting the capability of quantum machines to easily perform computations that are in principle unfeasible using classical computers [5, 6]. Other works have instead focused on "quantum data", i.e., information embedded in quantum states or quantum channels.

For the latter case, a fundamental model with particular relevance is that of quantum channel discrimination. This is known to have non-trivial implications for quantum sensing [16], in tasks such as the detection of targets [17–19] or the readout of memories [20, 21]. Recently, it has been applied to study the model of channel position finding [22], associated with absorption spectroscopy [23], and more sophisticated problems of barcode decoding and pattern recognition [10]. Here the use of quantum sources was shown to drastically reduce the error affecting the supervised classification of images, even when the output measurements are not optimized.

It is important to observe that, in most of the previous literature, the quantum models were optimized to reduce the classification error over training data, and then the generalization capabilities of the model were empirically verified by computing the classification error over a testing set. Some theoretical bounds were studied in [12, 24, 25], but only for particular classifiers. Intuitively, good quantum models should closely cluster data into well separated regions of the embedding Hilbert space [7] and only use a small, yet sufficiently large subspace of the full Hilbert space.

For this reason, in this manuscript we formally study the generalization capabilities of quantum models, and in particular of quantum embeddings, using tools from quantum information theory. Generalization aims to answer the following question: *After having trained the model using a few known examples, can the model accurately classify unseen data?* We will show how to define the complexity of quantum models using entropic quantities, which allow us to assess generalization. From the study of these quantities, we will show how different properties of the quantum embedding affect the classification accuracy and generalization, such as the dimension of the Hilbert space, the amount of noise, and the amount of neglected information via, e.g., pooling layers. Our results are based on the study of the linear loss function, which links quantum machine learning to quantum decision theory [26]. Nonetheless, we show how similar conclusions can be obtained in a loss-independent framework, by generalizing the information bottleneck principle [27] to quantum embeddings.

Our paper is organized as follows. In Sec. II we formally define different quantum classification tasks and study different training and testing errors as a function of quantum information quantities, for binary classification problems. In Sec. III we introduce a quantum version of bias-variance tradeoff, which defines fundamental limitations on the testing error for finite amounts of data; we also formally study how to reduce these errors using carefully designed quantum models. Conclusions are drawn in Sec. IV. The mathematical derivations of our results, as well as the extension to multi-ary classification, are presented in Appendix A.

## II. QUANTUM INFORMATION BOUNDS FOR SUPERVISED LEARNING

We are interested in learning the unknown functional relation $c = f(x)$ between a set of inputs $x$ and outputs $c$.
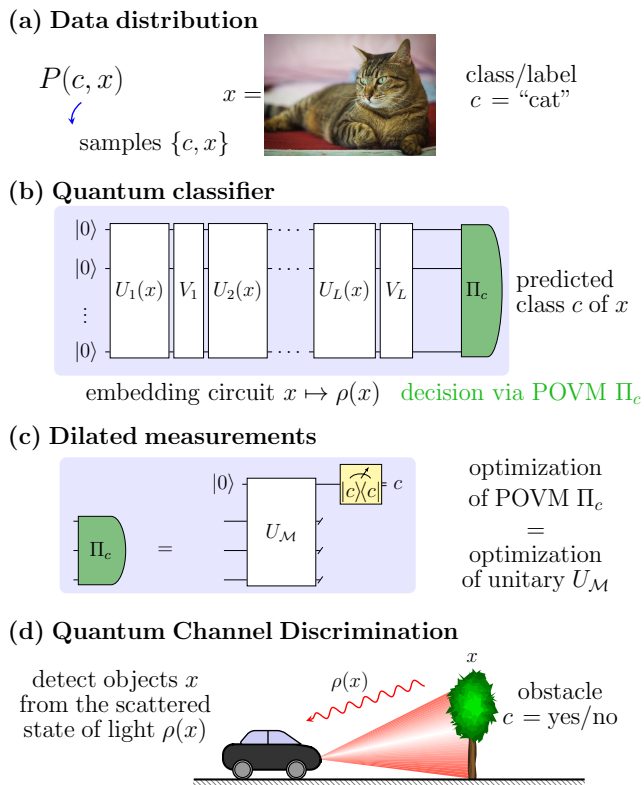
---

* leonardo.banchi@unifi.it

### (a) Data distribution

$P(c, x)$

$x =$



class/label
$c = $ "cat"

samples $\{c, x\}$

### (b) Quantum classifier



embedding circuit $x \mapsto \rho(x)$   decision via POVM $\Pi_c$

### (c) Dilated measurements



optimization
of POVM $\Pi_c$
=
optimization
of unitary $U_{\mathcal{M}}$

### (d) Quantum Channel Discrimination

detect objects $x$
from the scattered
state of light $\rho(x)$



obstacle
$c = $ yes/no

FIG. 1. (a) Example of an abstract data distribution $P(c, x)$, where $x$ describes images of animals and $c$ specifies the kind of animal, e.g., a cat. (b) General quantum classifier circuit with $L$ layers. The classical input $x$ is embedded into a quantum state $\rho(x)$ via layers of $x$-dependent and $x$-independent gates. A POVM $\{\Pi_c\}$ is performed at the end of the circuit. The predicted class of $x$ corresponds to the measurement outcome $c$. (c) Any POVM can be expressed as a unitary circuit followed by a projective measurement $|c\rangle\langle c|$ on a suitably large ancillary system. (d) In quantum channel discrimination, the images $x$ live in the physical world; a quantum probe senses the outside world and $\rho(x)$ is the scattered state of light collected by the detector, which depends on the outside objects. The detector then classifies the image with a POVM, as in (c).

Here we consider a classification task where each output $c$ is the predicted class of $x$. Following common practices in theoretical machine learning, we assume that all possible pairs of data $(c, x)$ follow some unknown probability distribution $P(c, x)$, so data pairs are independent samples from $P$ (see Fig. 1a). For simplicity we focus on inputs $x$ made of images and introduce two different approaches where quantum mechanics is used to classify them. In the first one, shown in Fig. 1b, images are initially saved in a classical digital memory, and classification is done by first *embedding* a classical image $x$ into a quantum state $\rho(x)$, via a circuit whose gates depend on $x$, and then by applying a measurement, described by a positive-operator valued measure (POVM) $\{\Pi_c\}$, whose outcome $c$ is the model's prediction for the class of $x$. Via Naimark's dilation theorem, such a POVM can be

effectively implemented as shown in Fig. 1c, namely by using an ancillary system whose Hilbert space dimension is equal to the number $N_C$ of classes, by first applying a unitary circuit that couples the state and the ancilla, and then performing a projective measurement $|c\rangle\langle c|$ on the ancillary system. The quantum classifier is probabilistic: given an image $x$ the predicted class $c$ is found with probability $p_Q(c|x) = \text{Tr}[\Pi_c \rho(x)]$. A deterministic classifier can be built using different techniques of quantum decision theory [26], for instance by repeating the measurement many times and taking the most likely class, or by defining an observable $\mathcal{M} = \sum_c m_c \Pi_c$, for certain real numbers $m_c$, and then assigning a certain class depending on the expectation value $\text{Tr}[\mathcal{M}\rho(x)]$. For instance, for binary classification problems with $c = \{0, 1\}$ we may set $m_0 = -1$, $m_1 = 1$ and then assign the class depending on the sign of $\text{Tr}[\mathcal{M}\rho(x)]$ [7]. The embedding circuit, with $x$-dependent and $x$-independent gates $U_i(x)$ and $V_j$, in Fig. 1b, together with the POVM $\{\Pi_c\}$ define the *model*, which may be optimized during training. In most of the studies available in the literature, the embedding gates $U_i(x)$ and $V_j$ are fixed by design, and the only optimization is over the last unitary $U_M$, which defines the POVM. On the other hand, in quantum metric learning [7], the optimal POVM is analytically constructed from either Helstrom measurements [28] or the SWAP test, and the optimization is over the embedding circuit only.

A mathematically related, yet physically different problem consists in classifying *physical* objects using quantum sensors, as in the example shown in Fig. 1d. There, $\rho(x) = \mathcal{E}_x[\rho_{\text{in}}]$ describes the state received by a quantum detector, where $\rho_{\text{in}}$ is input probe state of light, possibly entangled, and $\mathcal{E}_x$ describes how the photons are scattered depending on the objects $x$ living in the physical world. Here, $\rho_{\text{in}}$ and $\{\Pi_c\}$ define the model, while $\mathcal{E}_x$ is fixed.

To reliably classify either digital or physical images, we should formally understand how to define the optimal embedding $x \mapsto \rho(x)$ and/or POVMs in order to reduce the classification error, namely the difference between the predicted and true class of $x$. However, since these optimal choices are learnt from data, the crucial question is generalization. In the next sections we use tools from quantum information theory to formally study the two main errors, namely the approximation and generalization errors, which rigorously formalize the empirical testing error (see Fig. 2). We will study how different properties of the embedding affect accuracy or generalization, as schematically shown in Fig. 3, and fundamental limitations about the errors that we may expect for a given data distribution and for finite training samples.

### A. Training and testing with linear loss

In this section we discuss the various sources of error that may prevent generalization. Readers already famil-
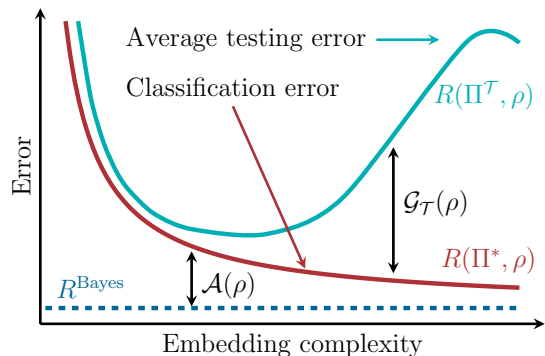
FIG. 2. Summary of the error sources for a fixed embedding $x \mapsto \rho(x)$ and a finite number of training samples. The classification error $R(\Pi^*, \rho)$ is the average loss with the unknown optimal measurement $\Pi^*$. The average testing error $R(\Pi^{\mathcal{T}}, \rho)$ replaces $\Pi^*$ with the POVM $\Pi^{\mathcal{T}}$ estimated from the training set $\mathcal{T}$ via empirical risk minimization. The testing error $R_{\mathcal{T}'}(\Pi^{\mathcal{T}}, \rho)$ is a finite sample approximation of $R(\Pi^{\mathcal{T}}, \rho)$ over the testing set $\mathcal{T}'$. The difference between the average testing error and the Bayes risk $R^{\mathrm{Bayes}}$ is split into the approximation error $\mathcal{A}(\rho)$ and the generalization error $\mathcal{G}_{\mathcal{T}}(\rho)$. The training error typically behaves as $R(\Pi^*, \rho)$.
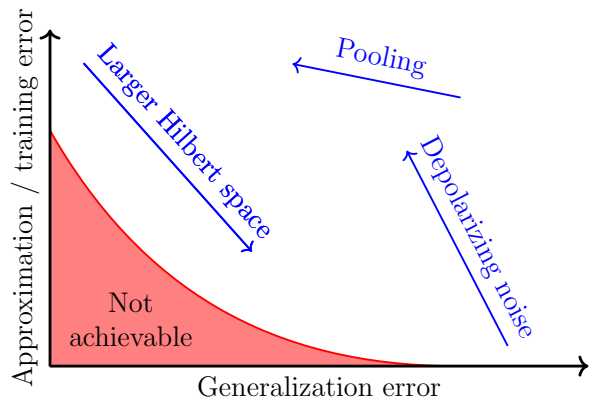


FIG. 3. Summary of some of the main conclusions of this paper. The approximation and generalization errors are mathematically related, respectively, to the training and testing error over some datasets, and they cannot be simultaneously minimized (bias-variance tradeoff). We use quantum information quantities to bound these errors and show how they are affected by the dimensionality of the Hilbert space embedding, noise, and "information pooling".

iar with this topic may skip this section and refer to Fig. 2 for the notation.

In supervised learning the available data are split between a training and a testing set. Both these sets are composed of pairs $(c_k, x_k)$, namely images $x_k$ and their true class $c_k$, but are used differently. We consider the training set $\mathcal{T} = \{(c_k, x_k)\}_{k=1,\dots,T}$ with $T$ pairs, and similarly a testing set $\mathcal{T}'$ with $T'$ pairs. In the training part a model is optimized in order to minimize a suitable distance between the true class $c$ and the predicted class

for all possible pairs $(c, x) \in \mathcal{T}$ in the training set. For a fixed quantum embedding $x \mapsto \rho(x)$ and POVM $\{\Pi_c\}$ the quantum model predicts a class $\tilde{c}$ with probability $\mathrm{Tr}[\Pi_{\tilde{c}}\rho(x)]$. If $c$ is the true label of $x$, we may define a linear *loss* as the probability of misclassification, namely the probability that the predicted class $\tilde{c}$ is different from the true class $c$

$$\ell(c, x) = \sum_{\tilde{c} \neq c} \mathrm{Tr}[\Pi_{\tilde{c}}\rho(x)] = 1 - \mathrm{Tr}[\Pi_c\rho(x)], \qquad (1)$$

where the second equality follows from $\sum_c \Pi_c = \mathbb{1}$. As we will see, the linear loss allows us to link quantum machine learning with quantum information and quantum decision theory [26].

Training is normally done via empirical risk minimization, where the empirical risk is the average loss over all possible pairs $(c_k, x_k)$ of the training set, and the minimization is over the parameters of the model, namely the POVM and embedding; in our case,

$$R_{\mathcal{T}}(\Pi, \rho) = \frac{1}{T} \sum_{(c_k, x_k) \in \mathcal{T}} \ell(c_k, x_k). \qquad (2)$$

In general such minimization does not have an analytic solution, except for a few notable cases. For binary classification problems, where $c = \{0, 1\}$ can only have two distinct values, and fixed embeddings, the optimal $\mathcal{T}$-dependent POVM, $\Pi^{\mathcal{T}} = \mathrm{argmin}_{\Pi}[R_{\mathcal{T}}(\Pi, \rho)]$, is the Helstrom measurement [28], which is extensively used in quantum hypothesis testing and quantum state discrimination. The Helstrom measurement operator $\Pi_0^{\mathcal{T}}$ ($\Pi_1^{\mathcal{T}}$) is the projection onto the eigenspace of positive (negative) eigenvalues of $\frac{T_0}{T}\rho_0^{\mathcal{T}} - \frac{T_1}{T}\rho_1^{\mathcal{T}}$, where $T_c$ is the number of images in the training set with class $c$ and $\rho_c^{\mathcal{T}}$ is a mixture of all the states $\rho(x)$ with inputs in $\mathcal{T}$ and fixed class $c$. Although not necessary, to simplify the equations we will always assume that the training set contains an equal number of images per class, so $T_c/T = 1/2$. Using the optimal Helstrom measurement the minimum empirical risk can be written analytically in terms of the trace distance between the two average states $\rho_0^{\mathcal{T}}$ and $\rho_1^{\mathcal{T}}$

$$R_{\mathcal{T}}(\Pi^{\mathcal{T}}) = \frac{1}{2}\left(1 - \frac{1}{2}\|\rho_0^{\mathcal{T}} - \rho_1^{\mathcal{T}}\|_1\right). \qquad (3)$$

For fixed embeddings, the above quantity is what defines the *training error*, namely the average loss over the training set. From the above equation, zero training error is only possibly when $\|\rho_0^{\mathcal{T}} - \rho_1^{\mathcal{T}}\|_1 = 2$, which happens when $\rho_0^{\mathcal{T}}$ and $\rho_1^{\mathcal{T}}$ have orthogonal support. We will show in Appendix. A that similar conclusions also hold when the number of classes is greater than two.

Does the model generalize? Empirically we need to check how the model performs with images not present in the training set. This is normally done by studying the testing error $R_{\mathcal{T}'}(\Pi^{\mathcal{T}}, \rho)$, which is similar to Eq. (2), but where the samples are taken from the testing set $\mathcal{T}'$. In

order to define the generalization error more formally, we need first to define the true average classification error

$$R(\Pi, \rho) = \mathop{\mathbb{E}}_{(c,x) \sim P} \ell(c, x) = 1 - \sum_c P(c) \operatorname{Tr}[\Pi_c \rho_c], \quad (4)$$

where in the last expression we use the chain rule $P(c, x) = P(x|c)P(c) = P(c|x)P(x)$, $P(x) = \sum_c P(c, x)$, $P(c) = \sum_x P(c, x)$ and we define the average quantum embedding as

$$\rho_c = \sum_x P(x|c)\rho(x). \quad (5)$$

The training error (2) is an empirical approximation of the classification error (4) where the formal average over all possible pairs $(c, x)$ is substituted with a finite average over the training set. The optimal classification POVM, $\Pi^* = \operatorname{argmin}_\Pi R(\Pi, \rho)$, is in general different from the $\Pi^\mathcal{T}$ that we get from empirical risk minimization. Overfitting happens when this difference is significant, namely when $\Pi^*$ and $\Pi^\mathcal{T}$ disagree on the class of an image not present in the training set. For a fixed embedding, the generalization error, also called the *estimation error*, is defined as $R(\Pi_\mathcal{T}, \rho) - R(\Pi^*, \rho)$, namely as a difference between two classification errors, where in one case we use the true classifier and in the other we use the classifier built from the training set $\mathcal{T}$. Notice that the testing error $R_{\mathcal{T}'}(\Pi^\mathcal{T}, \rho)$ is an empirical approximation of $R(\Pi_\mathcal{T}, \rho)$.

In order to have a low testing error, we need to have both a low generalization error and a low classification error $R(\Pi^*)$. The lowest possible classification error can be achieved via the Bayes classifier, and is therefore called $R^{\text{Bayes}}$. The difference between the average testing error $R(\Pi_\mathcal{T}, \rho)$ and $R^{\text{Bayes}}$ can be written as

$$R(\Pi_\mathcal{T}, \rho) - R^{\text{Bayes}} = \mathcal{G}_\mathcal{T}(\rho) + \mathcal{A}(\rho), \quad (6)$$

with

$$\mathcal{G}_\mathcal{T}(\rho) = R(\Pi_\mathcal{T}, \rho) - R(\Pi^*, \rho), \quad (7)$$
$$\mathcal{A}(\rho) = R(\Pi^*, \rho) - R^{\text{Bayes}}. \quad (8)$$

In Eq. (6) we see that the difference between the average testing error and the Bayes risk can be split into two positive terms (see also Fig. 2): $\mathcal{G}_\mathcal{T}(\rho)$ is the previously defined generalization error while $\mathcal{A}(\rho)$ is called the *approximation error*. A standard result of statistical learning theory, dubbed the bias-variance tradeoff [29], shows that it is impossible to minimize both $\mathcal{A}$ and $\mathcal{G}$. Keeping a simple embedding to avoid overfitting may introduce a bias in the resulting predictions, while too complex embeddings lead to overfitting and a higher variance in the predictions. We remark that these complexity analyses cannot explain the success of deep learning, where models with millions of parameters generalize well in spite of their complexity. There are some explanations of why deep-learning works in particular models [30], but this is

still a subject of intensive research. Moreover, quantum models that can be trained in near-term quantum hardware are quite far from the regime where deep learning operates, so our conclusions are for models of "moderate complexity". In the next section, we will study bounds on the approximation and generalization error using tools from quantum information theory, and then we will discuss, in Sec. III, how different properties of the embedding affect these errors.

## B. Generalization error

Employing tools from statistical learning theory [29] and quantum information, in Appendix. A we show that, for a given embedding, with probability at least $1-\delta$, the generalization error is bounded as

$$G_\mathcal{T} \leq 2\sqrt{\frac{\mathcal{B}}{T}} + \sqrt{\frac{2\log(1/\delta)}{T}}, \quad (9)$$

where $T$ is the size of the training set,

$$\mathcal{B} = \left( \operatorname{Tr} \sqrt{\sum_x P(x)\rho(x)^2} \right)^2 = 2^{I_2(X:Q)} \quad (10)$$

depends on the embedding, and $P(x)$ is the (unknown) prior probability for an image $x$. We refer to $\mathcal{B}$ as the *generalization bound*, which constrains how large the generalization error can be for a fixed number $T$ of training pairs.

The inequality (9) applies to binary classification problems, but its general form, derived in Appendix. A, is equivalent to (9) up to a constant that depends on the number of (equiprobable) classes – see Theorem 1. The inequality (9), with the explicit form of $\mathcal{B}$ in (10), represents one of the central result of this section, as it links the generalization error to properties of the embedding that are measured by information theoretic quantities. Indeed, the quantity found in the second equality of Eq. (10) is the 2-Renyi mutual information between subsystems $X$ and $Q$ of the classical-quantum state

$$\rho_{CXQ} = \sum_{cx} P(c, x) |cx\rangle\langle cx| \otimes \rho(x). \quad (11)$$

For general $\alpha$ and subsystems $A$ and $B$, the $\alpha$-Renyi mutual information [31] is defined as

$$I_\alpha(A:B) = \frac{\alpha}{\alpha - 1} \log_2 \operatorname{Tr} \sqrt[\alpha]{\operatorname{Tr}_A \left( \rho_A^{\frac{1-\alpha}{2}} \rho_{AB}^\alpha \rho_A^{\frac{1-\alpha}{2}} \right)}. \quad (12)$$

For $\alpha \to 1$ one recovers the quantum mutual information $I_1(A:B) \equiv I(A:B) = H(A) + H(B) - H(AB)$, where $H(A) = S(\rho_A)$ and $S(\rho) = -\operatorname{Tr}[\rho \log_2 \rho]$ is the von Neumann entropy. Although $I_\alpha(A:B)$ for $\alpha \neq 1$ does not satisfy all of the properties of $I_1(A:B)$, it does satisfy the data processing inequality [31], which is a

central ingredient in quantum information theory. In Eq. (11) we have introduced three Hilbert spaces: the embedding space $Q$ where the states $\rho(x)$ live, the class space $C$ spanned by $\{|c\rangle\}_{c=1,\ldots,N_C}$ and the input space $X$ spanned by $\{|x\rangle\}$ for all possible values of $x$, namely where each input $x$ is mapped onto a different orthogonal state $|x\rangle$. For instance, if the images $x$ have $n$ pixels, each with a 16 bit color pattern, then $|x\rangle$ lives in a space of $4n$ qubits. For continuous inputs, one must consider a suitably-regularized infinite dimensional Hilbert space. Here for simplicity, we assume that $X$ is discrete and can be represented using $N_X$ classical bits, so $\rho_{CXQ}$ lives in a $N_C 2^{N_X+N_Q}$ dimensional Hilbert space.

Inequalities such as in (9) are common in statistical learning theory and show that a model generalizes well whenever $T \to \infty$. The importance of (10) is in quantifying when the size $T$ of the training set is "large". According to our analysis, a training set is large whenever $T \gg 2^{I_2(X:Q)}$, namely when $\log_2(T)$ is much larger than the number of bits required to describe the information shared between the input distribution and the quantum embedding, as measured by $I_2(X:Q)$.

### C.  Approximation error

In the last section, we formally optimized over the measurements, but we considered a fixed embedding $x \mapsto \rho(x)$. A similar restriction is applied in classical machine learning when the model class is fixed *a priori*, e.g., a neural network with a given architecture and a certain number of nodes. The difference between the minimum classification error that we may obtain with a given architecture and the theoretical minimum over all possible architectures, namely the Bayes risk, is the approximation error (8). For a known $P(c,x)$ and a given $x$, the Bayes classifier picks the class that maximizes $P(c|x)$. The corresponding Bayes risk for binary classification problems with $P(c) = 1/2$ is then

$$R^{\text{Bayes}} = 1 - \frac{1}{2}\sum_x \max\{P(x|0), P(x|1)\} = \frac{1-\Delta}{2},$$

where

$$\Delta = \frac{1}{2}\sum_x \big| P(x|0) - P(x|1) \big|. \qquad (13)$$

Using the definition of the approximation error (8) and the classification error $R(\Pi^*)$, which is analogous to (3) but with the states (5), we find that the approximation error for quantum binary classification problems can be written as

$$\mathcal{A} = R(\Pi^*) - R^{\text{Bayes}} = \Delta - \frac{\|\rho_0 - \rho_1\|_1}{2}. \qquad (14)$$

It is simple to show that $0 \leq \mathcal{A} \leq \Delta$. The upper bound is trivial, and can be achieved when $\rho_0 = \rho_1$. As for the

lower bound, defining $\rho_c^{XQ} = \sum_x P(x|c)|x\rangle\langle x| \otimes \rho(x)$, we first note by explicit calculation that $\|\rho_0^{XQ} - \rho_1^{XQ}\|_1 = 2\Delta$. Then by the contractivity of the trace distance over quantum channels we find $\|\rho_0^Q - \rho_1^Q\|_1 \leq \|\rho_0^{XQ} - \rho_1^{XQ}\|_1$, where $\rho_c^Q = \text{Tr}_X[\rho_c^{QX}] \equiv \rho_c$, thus showing that $\mathcal{A} \geq 0$.

In the previous section, we have showed how to bound the generalization error using the mutual information between subsystems $X$ and $Q$ in (11). We can use entropies to bound the average classification error $R(\Pi^*)$, and hence $\mathcal{A}$. Indeed, using the quantum Chernoff bound [32] and explicit calculations we get $R(\Pi^*) \leq \frac{1}{2}\text{Tr}[\sqrt{\rho_0}\sqrt{\rho_1}] = 2^{-I_{\frac{1}{2}}(C:Q)} - \frac{1}{2}$, which shows that a low classification error is possible when $I_{\frac{1}{2}}(C:Q)$ is large. A more general result, valid for any number of classes, can be found using conditional entropies [33],

$$R(\Pi^*) = 1 - 2^{-H_{\min}(C|Q)} \leq 1 - \frac{2^{I(C:Q)}}{N_C}, \qquad (15)$$

which is valid for states of the form given in Eq. (11), where $H_{\min}(C|Q) \leq H(C|Q)$ is the min- conditional entropy, which is smaller than von Neumann's conditional entropy [34]. The second inequality comes from $H(C|Q) = H(C) - I(C:Q)$ and $H(C) = \log_2 N_C$ for a classification problem with $N_C$ classes. Since $Q$ and $C$ are classically correlated, $I_1(C:Q) \leq H(C)$ and a small risk is possible when the mutual information between $Q$ and $C$ is large.

In the following section, we build upon the approximation and generalization errors to study how to define *good* embeddings for reliable classification.

### III.  BIAS VARIANCE TRADEOFF FOR QUANTUM MACHINE LEARNING

The bias-variance tradeoff is a central result in machine learning that states that it is impossible to minimize both the approximation and the generalization errors. If a model has lots of parameters and structure, one would expect low approximation error, potentially at the cost of poor generalization (overfitting). On the other hand, a low-dimensional model with few parameters would be easier to learn, but it might not reliably classify the data. Modern deep learning challenges this classical picture [30], as neural networks with millions of parameters, trained with huge amounts of data, can both display small training and testing errors.

We study the bias-variance tradeoff using quantum information. Remember that the difference between the average testing error and the Bayes risk can be written as a sum of two positive terms (6), the generalization error $\mathcal{G}$ and the approximation error $\mathcal{A}$. The latter is the difference between the average classification error $R$ and the Bayes risk, while the former can be bounded by the generalization bound $\mathcal{B}$ from (10), and can be made arbitrarily small by considering arbitrarily large training sets with $T \to \infty$. For finite and fixed $T$, we show that it is

impossible to minimize both $\mathcal{A}$ and $\mathcal{G}$, so a *good* quantum embedding $x \mapsto \rho(x)$ is always a compromise between approximation and generalization, as schematically shown in Fig. 3.

Many of the intuitive characterizations of good embeddings will be formally derived in the next section, using tools from quantum information. We will use, in particular, the contractivity of the trace distance under quantum channels $\mathcal{E}^{Q \to Q'}$ [35] mapping from the space $Q$ to the space $Q'$, i.e., $\|\mathcal{E}^{Q \to Q'}(\rho - \sigma)\|_1 \leq \|\rho - \sigma\|_1$, the data processing inequality [31] $I_2(X{:}Q) \geq I_2(X{:}Q')$, and finally the bounds satisfied by $\mathcal{B}$, which are studied in Appendix A

$$1 \leq \mathcal{B} \leq 2^{\min\{H_2(X), N_Q\}}, \qquad (16)$$

where $D = 2^{N_Q}$ is the dimension of the embedding Hilbert space, i.e., $N_Q$ is the number of qubits in the quantum embedding, and $H_\alpha[X] = \frac{\alpha}{\alpha-1} \log_2[\sum_x P(x)^{\frac{1}{\alpha}}]$, is the Rényi entropy of the classical image distribution.

### A. Properties of quantum embeddings

*It is impossible to minimize both $\mathcal{B}$ and $R$*: A good embedding discards all the *irrelevant* information from the input space $X$ that is not necessary to predict the class $C$. Indeed, according to Eqs. (10) and (15), $I_2(X{:}Q)$ must be small while $I(C{:}Q)$ must be large. We will show that it is impossible to minimize both $\mathcal{B}$ and $R$ by studying the two extreme cases where the information about $X$ is either fully discarded or fully maintained.

*Constant embeddings provide zero generalization error, but the largest approximation error*: indeed, the generalization error (7) is defined as the distance between the risk obtained by minimizing the empirical loss over the training data and the true average loss. For constant embeddings this difference is zero: if we restrict ourselves to classifiers that always produce a constant answer, then it is trivial to learn this classifier from data, but the average classification error will be as high as 50%. Mathematically, from the definition (10) and the bounds (16), it is clear that the minimum $\mathcal{B}$ is achieved with the trivial constant embedding, $\rho(x) = \rho$ for all $x$, but such a trivial embedding provides both the largest $R = 1/2$ and the largest training error $R_{\mathcal{T}} = 1/2$ from Eq. (3). Moreover, using mutual informations, the constant embedding is the only embedding for which the space $Q$ is uncorrelated from both $C$ and $X$ in (11) and so $I(X{:}Q) = I(C{:}Q) = 0$.

*Basis encoding guarantees zero approximation error, but the largest generalization error*. Basis encoding [2, 36] is defined as $\rho(x) = |x\rangle\langle x|$, namely different inputs are mapped onto orthogonal vectors on a suitably large Hilbert space. No information is lost, or hidden, in the quantum embedding, so using Eqs. (14) and (16), we get the lowest possible approximation error $\mathcal{A} = 0$, meaning the average loss can achieve the Bayes risk. However, for the same reason, we also get the largest $\mathcal{B} = 2^{H_2(X)}$, since
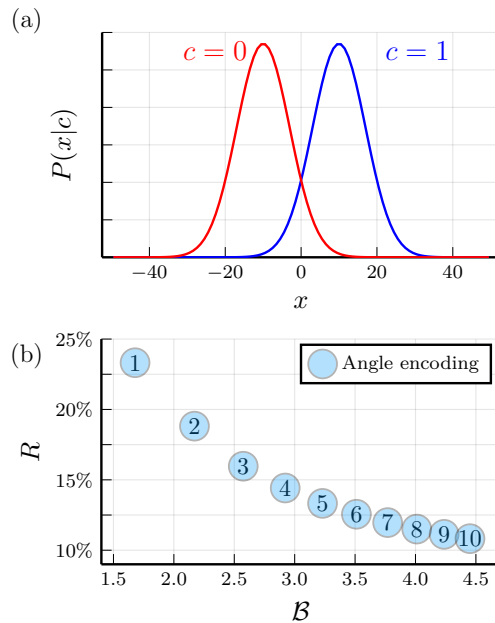


FIG. 4. (a) Example data distributions for two different classes $c = \{0, 1\}$: Gaussian distributions with different means $\pm 10$ and the same standard deviation 7. The corresponding Bayes risk is $R^{\mathrm{Bayes}} \simeq 7.6\%$. (b) Average classification error $R$ (4) vs generalization bound $\mathcal{B}$ (10) for the angle encoding $\rho(x) = |\psi(x)\rangle\langle\psi(x)|^{\otimes N_Q}$ where $|\psi(x)\rangle = \cos(x/2)|0\rangle + \sin(x/2)|1\rangle$ and the $x$-values have been normalized such that $x \in [0, 2\pi]$. The number inside each circle represents the value of $N_Q = 1, \ldots, 10$.

$X = Q$. Therefore, basis encoding allows us to reach the theoretical minimum classification error, but it requires a large embedding space and many $(T \gg \mathcal{B})$ training pairs to avoid overfitting.

*High-dimensional embeddings may have lower approximation error*: in Appendix A (Theorem 2) we show that if we define an embedding by taking $N$ copies of a simpler one, i.e., if we consider $x \mapsto \rho(x)^{\otimes N}$, then $\mathcal{A} \to 0$ for $N \to \infty$ as long as $F(\rho(x), \rho(y)) \neq 0$ for $x \neq y$, where $F(\rho, \sigma) = \|\sqrt{\rho}\sqrt{\sigma}\|_1$ is the fidelity between two quantum states. If $\rho(x)$ is an $N_Q$ qubit state, then optimized embeddings using $N \times N_Q$ qubits can only have a lower approximation error than $\rho(x)^{\otimes N}$, since the latter is a particular case. However, high dimensional embeddings may suffer from poor generalization, as $\mathcal{B}$ may be larger. A numerical check of this prediction is shown in Fig. 4 for a binary discrimination problem with Gaussian priors. We see that, as the number of qubits increases, the classification error risk quickly decreases but the generalization bound increases. This is consistent with our numerical prediction. According to Theorem 2, for many-copies, $\mathcal{A}$ decreases exponentially with $N$. Moreover, for local observations $I(X{:}Q)$ only increases logarithmically with $N$ [37, 38], meaning $\mathcal{B}$ increases linearly with $N$, as we observe numerically.

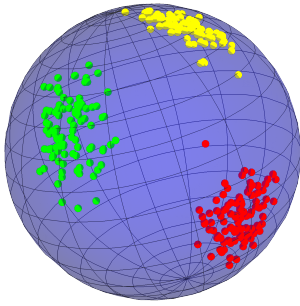*Low-entropy datasets and low-dimensional embeddings*

FIG. 5. Geometric visualization of a good embedding, where each point in the sphere represents a state. Points belonging to different classes are plotted with different colors. A good embedding should cluster points with the same class and separate points belonging to different classes.

*can in principle generalize well*: this is a trivial consequence of (16), when the entropy of the datasets is measured by $H_2[X]$. The statement about the dimension can be made a bit more precise by focusing not just on the dimension of the Hilbert space, but on how much the information is distributed within the Hilbert space. For instance, let us assume a pure state embedding $\rho(x) = U(x)|0\rangle\langle 0|U(x)^\dagger$ with a unitary embedding circuit $U(x)$. If the embedding is such that the input information is "fully-scrambled" in a $d$-dimensional subspace, with $d \ll 2^{N_Q}$, then we may write $\sum_x P(x)\rho(x)^2 \approx \mathbb{1}_d/d$. Substituting this approximation in (10) we get

$$\mathcal{B} \approx \mathcal{O}(d) . \quad (17)$$

Therefore, a good embedding for generalization is not necessarily built using few qubits, but rather it is optimized to "scramble" information in a small subspace of the full $N_Q$-qubit Hilbert space.

*Geometric characterization*: There is an intuitive geometrical characterization of good embeddings (see e.g., Ref. [7]). A good embedding is possible when the fidelity between two embedded states is small if the inputs are from different classes and high if the inputs are from the same class, as schematically shown in Fig. 5 . Indeed, using the Fuchs-van de Graaf inequality and the strong concavity of the fidelity, we get

$$\mathbb{E}_{\mathcal{T}} R_{\mathcal{T}}(\Pi^{\mathcal{T}}) \leq \frac{1}{2}\mathbb{E}_{\mathcal{T}}\left[F(\rho_0^{\mathcal{T}}, \rho_1^{\mathcal{T}})\right] \leq \frac{1}{2}F(\rho_0, \rho_1), \quad (18)$$

so, on average, low training errors and low classification errors are possible when the fidelity between the two averaged states $\rho_0$ and $\rho_1$ is small. Moreover, in Appendix (A) we show that $\mathcal{B} \leq (\sum_c \sqrt{P(c)\mathcal{B}_c})^2$ and, for pure state embeddings,

$$\mathcal{B}_c \leq 1 + \sqrt{(r_c^2 - r_c)(1 - \mathrm{Tr}[\rho_c^2])}. \quad (19)$$

where $r_c$ is the rank of $\rho_c$. The general case is discussed in Appendix (A). The above inequality shows that low generalization error is possible when the average embedding

states $\rho_c$ have low rank and/or high purity. Since $\rho_c$ is an ensemble of embeddings for inputs from the same class, the above requirement is satisfied when $\rho(x)$ maps all the inputs from the same class to the same state. More precisely, for pure state embeddings $\rho(x) = U(x)|0\rangle\langle 0|U(x)^\dagger$, the purity can be written as

$$\mathrm{Tr}[\rho_c^2] = \sum_{x,y} P(x|c)P(y|c)F(\rho(x), \rho(y))^2, \quad (20)$$

where $F(\rho(x), \rho(y)) = |\langle 0|U(y)^\dagger U(x)|0\rangle|$ is the fidelity. Therefore, good generalization is possible whenever $F(\rho(x), \rho(y))$ is large for all possible pairs $(x, y)$ of inputs with the same class, namely when $\rho(x)$ and $\rho(y)$ are always geometrically close in the embedding Hilbert space. Combining this with (18) we see that a desirable feature to get a good embedding is that the fidelity between two embedded states is small if the inputs are from different classes and high if the inputs are from the same class, as in Fig. 5.

*Noisy operations*: We focus on what happens when $\rho(x) = (1 - \epsilon)U(x)|0\rangle\langle 0|U(x)^\dagger + \epsilon\mathbb{1}/2^{N_Q}$, namely when the embedding discussed in the previous example is degraded by depolarising noise with strength $\epsilon$. Again assuming that the average fully scrambles information in a $d$-dimensional subspace, then

$$\sum_x P(x)\rho(x)^2 \approx \left[(1 - \epsilon)^2 + \frac{2(1 - \epsilon)\epsilon}{2^{N_Q}}\right]\frac{\mathbb{1}_d}{d} + \frac{\epsilon^2}{2^{2N_Q}}\mathbb{1},$$

from which

$$\mathcal{B} \approx \left(\sqrt{d}(1 - \epsilon + \epsilon/2^{N_Q}) + (1 - d/2^{N_Q})\epsilon\right)^2 \simeq d(1 - \epsilon)^2.$$

From the above equation, we see that the generalization error does not increase with noise. It actually decreases when $1 \ll d \ll 2^{N_Q}$, as for large $\epsilon$ the embedding approaches the constant embedding, which has the lowest generalization error but the highest classification and approximation errors.

*Pooling may help*: We have seen that a large embedding Hilbert space may favour the classification accuracy, yet hinder generalization. According to (16) the generalization bound may approach its largest value when $N_Q$, i.e., the number of qubits in the embedding, is as large as $H_2(X)$. What about the minimum number of qubits? For binary classification problems a good embedding can be obtained even with $N_Q = 1$. Indeed, the simplest embedding that achieves the minimum Bayes risk is $\rho^{\mathrm{Bayes}}(x) = |\tilde{c}\rangle\langle\tilde{c}|$, where $\tilde{c} = \arg\max_c P(x|c)$ is, for a given $x$, the class with largest conditional probability. Clearly it is impossible to construct this embedding, as the probabilities $P(x|c)$ are unknown, but the above example shows that a good embedding is possible with a single qubit. However, even though the state before the measurement must be as low-dimensional as possible, we may start from a large dimensional embedding and then iteratively *throw away information*, either via measuring some qubits and then applying a different unitary on

the remaining ones depending on the measurement result or, equivalently, by applying a conditional gate and then discarding some qubits via a partial trace.

Since the generalization error depends only on the dimension of the final Hilbert space, one can use pooling to iteratively reduce the number of qubits, using different layers, eventually leaving a single qubit for measurements. Promising forms of pooling have been proposed as a basis for Quantum Convolutional Neural Networks (QCNN) [8, 39], where the pooling layers are constructed using a reverse Multiscale-Entanglement-Renormalization-Ansatz (MERA) circuit, whose depth depends logarithmically on the total number of qubits. QCNNs have some desirable features, such as the ability to distinguish states corresponding to complex phases of matter [8], and the lack of barren plateaus in their parameter landscape [40], which aids training. Our analysis shows that QCNNs, or other embeddings built by iteratively pooling information, also have good generalization capabilities.

### B. Quantum Information Bottleneck

In the previous section we showed that it is impossible to minimize both the approximation and the generalization errors, when these are defined starting from the linear loss (1). We now show how the generalization/approximation tradeoff can also be understood from information theoretic principles that are independent of the choice of loss function. In classical settings, a method designed for this purpose is the information bottleneck (IB) principle [27, 41], which allows us to find the "best" compressed representation $Z$ of the input $X$ that nonetheless has all the relevant information required to predict the class $C$. The amount of compression can be quantified using the classical mutual information $I(X:Z)$, while $I(C:Z)$ quantifies the residual information between $C$ and $Z$. In order to have accurate classification $I(C:Z)$ must be large, while to have good compression $I(X:Z)$ must be small. The information bottleneck principle finds a compromise between accuracy and compression by minimizing the Lagrangian $\mathcal{L}_{IB} = I(X:Z) - \beta I(C:Z)$ for a certain value of $\beta$. The parameter $\beta$ allows us to *explore* different regimes and to favour either accuracy or compression. When $\beta = 0$ the minimization of $\mathcal{L}_{IB}$ achieves the best compression, without caring about correct classification. While for $\beta \to \infty$ the minimization of $\mathcal{L}_{IB}$ achieves optimal classification without compression. Quantum generalizations of the information bottleneck principle were considered for quantum communication problems in [42, 43]. Here we apply the IB principle to the different problem of finding the optimal embedding.

We focus on the state (11) where $X$ and $C$ are, respectively, the classical spaces of inputs and classes, and $Q$ is the quantum embedding Hilbert space. The quantum IB Lagrangian is then defined as

$$\mathcal{L}_{IB} = I(X:Q) - \beta I(C:Q), \qquad (21)$$

where $I(A:B) = I_{\alpha \to 1}(A:B)$ in (12) is the quantum mutual information. Both $I(X:Q)$ and $I(C:Q)$, can be expressed using Holevo's accessible information [44]. In (9), (10) and (15), we have shown that good generalization is possible whenever $I_2(X:Q)$ is small, while low classification error is possible when $I(C:Q)$ is large. These conclusions were found for the linear loss (4). We may assume that $I_\alpha(X:Q)$ define a family of generalization bounds for a particular loss function, so the minimization of the generalization error is consistent with the minimization of $I(X:Q)$, according to some metric, while the maximization of $I(C:Q)$ is consistent with the accurate prediction of $C$ from $Q$. For a particular value of $\beta$, the optimal embedding is then obtained as $\min_{\rho(x)} \mathcal{L}_{IB}$. From the definition, we find the explicit form of the IB Lagrangian as

$$\mathcal{L}_{IB} = (1-\beta)S\left[\sum_x P(x)\rho(x)\right] - \sum_x P(x)S[\rho(x)] +$$
$$+ \beta \sum_c P(c)S[\rho_c] + \sum_x \tilde{\lambda}_x \operatorname{Tr}[\rho(x)] + \eta , \quad (22)$$

where $S[\rho]$ is the von Neumann entropy of $\rho$, $\tilde{\lambda}_x$ are Lagrange multipliers to force correct normalization, and $\eta$ contains all the terms that are independent of the embedding. The optimal embedding corresponds to a minimum of $\mathcal{L}_{IB}$, which satisfies $\frac{\partial \mathcal{L}_{IB}}{\partial \rho(z)} = 0$. By explicit computation we find that the above condition defines a recursive equation for the optimal embedding

$$\tilde{\lambda}_z \rho(z) = e^{(1-\beta)\log \bar{\rho} + \beta \sum_c P(c|z) \log \rho_c}, \qquad (23)$$

where $\bar{\rho} = \sum_c P(c)\rho_c$ and $\lambda_z$ is directly related to $\tilde{\lambda}_z$ and is needed to enforce normalization. Alternatively, by restricting to pure state embeddings $\rho(x) = |\psi(x)\rangle\langle\psi(x)|$, we get

$$\tilde{\lambda}_z |\psi(z)\rangle = e^{(1-\beta)\log \bar{\rho} + \beta \sum_c P(c|z) \log \rho_c} |\psi(z)\rangle. \qquad (24)$$

From Eqs. (23) and (24) we see that, for $\beta = 0$, we get a constant embedding, while for large $\beta$ the optimal embedding for a given $x$ is iteratively obtained from one of the eigenvectors of $\sum_c P(c|x) \log \rho_c$ with the largest eigenvalue, or a mixture of them.

A numerical solution of the IB equations is shown in Fig. 6, where "pure" and "mixed" refer to either (24) or (23), which were solved for two Gaussian distributions and a single-qubit embedding, using a fixed number of iterations (1000). The Bayes risk is plotted as a reference, giving the smallest possible value of $R$ that can be obtained with any embedding. For a fixed $1 \le \beta \le 3$, we first compute the optimal embedding via either (24) or (23), and then compute the classification error $R$ from Eq. (4) and the generalization bound $\mathcal{B}$ from Eq. (10). Recall that, for a given $P(c, x)$, the classification error is equivalent to the approximation error $\mathcal{A}$, up to the constant Bayes risk (8). Fig. 6(a) shows the approximation-generalization tradeoff for the different regimes that we
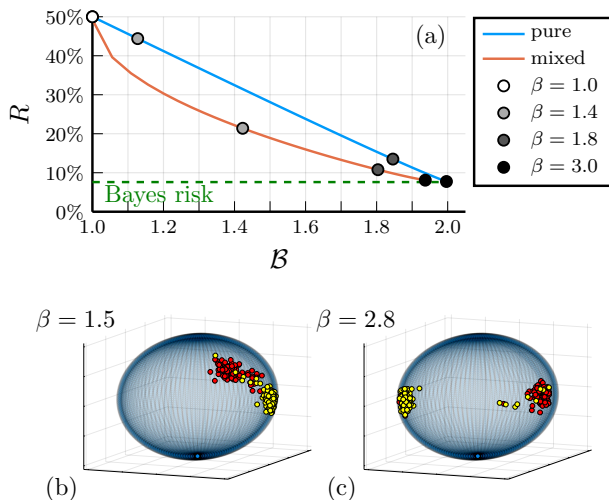
FIG. 6. (a) Average risk (approximation error) $R$ (4) vs. generalization error $\mathcal{B}$ (10) for the optimal embeddings obtained by solving the IB equations using either pure (24) or mixed (23) single-qubit states for different values of $\beta \in [1, 3]$. Some values of $R$ and $\mathcal{B}$ for particular $\beta$ are also shown with markers. (b) and (c) Bloch sphere visualization of the quantum embeddings $\rho(x)$ for different values of $x$ sampled from either $P(x|0)$ (red) or $P(x|1)$ (yellow), obtained by solving the IB equations (24) for single-qubit encodings, using the two shown values of $\beta$. In all three subfigures, the data distributions are those of Fig. 4(a).

have explored by varying $\beta$. For low values of $\beta$, we get an almost constant embedding with a large classification error (up to 50%) and low $\mathcal{B}$, while for large values of $\beta \geq 2$, we find that $R$ approaches the theoretical lower bound (Bayes risk), but at the expense of a larger generalization error, as $\mathcal{B}$ gets close to the theoretical upper bound (16). We point out though that for this particular example, with a single-qubit embedding and two Gaussian priors, the generalization error is always low due to the bound (16).

The properties of the optimal embedding are shown in Figs. 6(b) and (c). In particular, in panel (b) we observe that data belonging to different classes are clustered, but not well separated from each other. On the other hand, for larger values of $\beta$, points belonging to different classes are typically very far apart in the Bloch sphere, though there are still some points in the wrong cluster. This prediction is consistent with the analysis of the fidelity between two different embeddings discussed in the previous section and sketched in Fig. 5: a good embedding is such that $F(\rho(x), \rho(y))$ is large whenever $x$ and $y$ belong to the same class and small otherwise.

## IV. CONCLUSIONS

We have introduced some measures of complexity that allow the quantification of the generalization and approx-

imation capabilities of quantum embeddings $x \mapsto \rho(x)$, when optimal measurements are performed on the system. One of the main results of this paper is the bound on the generalization error via the Rényi mutual information $I_2(X:Q)$ between the embedding space $Q$ and the classical input space $X$. Thanks to our bound, overfitting does not occur when the number of training pairs $T$ is much bigger than $2^{I_2(X:Q)}$. Moreover, we have shown how to bound the approximation error via the mutual information between the embedding space and the class space, then shown that the classification error approaches it lowest possible value (Bayes risk), when the embedding Hilbert space dimension is very large. Our bounds were obtained for the linear loss function, but different losses can be linked to the linear loss via bounds. Finally, we have introduced an information bottleneck principle for quantum embeddings, which is independent of the choice of loss function and allows us to explore different trade-offs between accuracy and generalization.

Our analysis can be applied to models of moderate complexity, such as those that can be trained with near-term quantum hardware. It is currently an open question to understand whether quantum classifiers of very-high complexity can mimic the generalization capabilities of classical deep learning.

## Appendix A: Extended derivation

### 1. Statistical Learning Theory

Here we show a brief overview of the tools from statistical learning theory [29] that we use throughout the manuscript. As in the previous chapters, we assume that there exists an abstract probability distribution that models the inputs and their corresponding classes $P(c, x)$. This distribution is obviously unknown, but by construction, the samples in the training set $\mathcal{T}$ are drawn independently from $P(c, x)$. Suppose now that we have built a classifier $h \in \mathcal{H}$, where $\mathcal{H}$ is the set of classifiers that we are considering. We may define the error due to misclassification via the loss function $\ell_h(c, x)$, which is zero if and only if $c$ is the correct class of $x$. Training is done by minimizing the empirical risk, namely the

average loss over the training set

$$R_{\mathcal{T}}(h) = \frac{1}{T} \sum_{k=1}^{T} \ell_h(c_k, x_k) \ , \tag{A1}$$

while the "true" risk of a classifier $h$ is given by

$$R(h) = \mathop{\mathbb{E}}_{(c,x) \sim P} [\ell_h(c, x)] \ . \tag{A2}$$

Supervised learning is practically done via empirical risk minimization, namely the optimal data driven classifier is obtained from

$$h_{\mathcal{T}} = \mathop{\mathrm{argmin}}_{h \in \mathcal{H}} R_{\mathcal{T}}(h) \ . \tag{A3}$$

The generalization error defines how $h_{\mathcal{T}}$ performs with unseen data, i.e., data not present in the training set. Formally the generalization error is then defined as $R(h_{\mathcal{T}}) - \inf_{h \in \mathcal{H}} R(h)$. Setting $h^* = \mathrm{argmin}_{h \in \mathcal{H}} R(h)$ as the true optimal classifier, we may bound the generalization error $\mathcal{G}$ as

$$\begin{aligned}
\mathcal{G} = R(h_{\mathcal{T}}) - R(h^*) = \qquad\qquad\qquad & \tag{A4} \\
= R(h_{\mathcal{T}}) - R_{\mathcal{T}}(h_{\mathcal{T}}) + R_{\mathcal{T}}(h_{\mathcal{T}}) - R_{\mathcal{T}}(h^*) & \\
+ R_{\mathcal{T}}(h^*) - R(h^*) & \\
\leq R(h_{\mathcal{T}}) - R_{\mathcal{T}}(h_{\mathcal{T}}) + R_{\mathcal{T}}(h^*) - R(h^*) & \\
\leq 2 \sup_{h \in \mathcal{H}} |R(h) - R_{\mathcal{T}}(h)| \ , & \tag{A5}
\end{aligned}$$

where in the first inequality we used the fact that $h_{\mathcal{T}}$ is optimal for $R_{\mathcal{T}}$, therefore $R_{\mathcal{T}}(h_{\mathcal{T}}) \leq R_{\mathcal{T}}(h^*)$. The upper bound is known as the uniform deviation bound. It represents the maximum deviation between the true and empirical risks, Eqs. (A1)-(A2), maximized over the possible classifiers.

The goal of statistical learning theory is to study how much larger the risk $R(h_{\mathcal{T}})$ is than the Bayes risk, namely $R^{\mathrm{Bayes}} = \inf_h R(h)$ where the infimum is over all possible hypotheses, not restricted to $\mathcal{H}$. Then by summing and subtracting $R(h^*)$ we get

$$R(h_{\mathcal{T}}) - R^{\mathrm{Bayes}} = \mathcal{G} + \mathcal{A} \tag{A6}$$

where $\mathcal{A} = R(h^*) - R^{\mathrm{Bayes}}$ is the approximation error, which depends on the hypothesis space $\mathcal{H}$. One of the central results of statistical learning theory is the following [29]: if $\ell$ has support in $[0, 1]$ then with probability at least $1 - \delta$ we have that

$$\mathcal{G} \leq 4\mathcal{C}_T(\mathcal{H}) + \sqrt{\frac{2 \log(1/\delta)}{T}} \ , \tag{A7}$$

where $\mathcal{C}_T(\mathcal{H})$ is the Rademacher complexity of $\mathcal{H}$, which is defined as

$$\mathcal{C}_T(\mathcal{H}) := \mathop{\mathbb{E}}_{\mathcal{T} \sim P^T} \mathop{\mathbb{E}}_{\boldsymbol{\sigma}} \left[ \sup_{h \in H} \frac{1}{T} \sum_{k=1}^{T} \sigma_k \ell_h(c_k, x_k) \right], \tag{A8}$$

where $\sigma_k$ is a random variable which can take two possible values, $\pm 1$, with the same probability $1/2$, and the notation $\mathcal{T} \sim P^T$ means that the $T$ elements in the training set $\mathcal{T}$ are sampled independently from the distribution $P$. From (A7) we see that if the Rademacher complexity of $\mathcal{H}$ decreases with $T$, then, for sufficiently large $T$, the model is able to generalize and correctly predict the class of a new input, not present in the training set $\mathcal{T}$.

## 2. Quantum Rademacher Complexity

Let us calculate the Rademacher complexity of the quantum loss function introduced in (1), for which it is clear from the definition that $0 \leq \ell(c_k, x_k) \leq 1$, as requested. For a fixed embedding, defining $\mathcal{P}$ as the set of all possible POVMs, the Rademacher complexity of this quantum classifier (1) is

$$\mathcal{C}_T(\mathcal{P}) := \mathop{\mathbb{E}}_{\mathcal{T} \sim P^T} \mathop{\mathbb{E}}_{\boldsymbol{\sigma}} \left[ \sup_{\{\Pi_c\} \in \mathcal{P}} \frac{1}{T} \sum_{k=1}^{T} \sigma_k \sum_{c \neq c_k} \mathrm{Tr}[\Pi_c \rho(x_k)] \right]$$

$$= \mathop{\mathbb{E}}_{\mathcal{T} \sim P^T} \mathop{\mathbb{E}}_{\boldsymbol{\sigma}} \left[ \sup_{\{\Pi_c\} \in \mathcal{P}} \frac{1}{T} \sum_{k=1}^{T} \sigma_k \mathrm{Tr}[\Pi_{c_k} \rho(x_k)] \right] \tag{A9}$$

where in the second line we used the second equality in Eq. (1), the fact that the constant term (from substituting in Eq. (1)) commutes with the sup and is averaged out by $\mathbb{E}_{\boldsymbol{\sigma}}$, and finally the fact that the minus sign can be removed by noting that $\boldsymbol{\sigma}$ and $-\boldsymbol{\sigma}$ have the same distribution. Let us define

$$Q_{c,\boldsymbol{\sigma}}^{\mathcal{T}} = \frac{1}{T} \sum_{k=1}^{T} \delta_{c,c_k} \sigma_k \rho(x_k) \ , \tag{A10}$$

then by linearity we may rewrite Eq. (A9) as

$$\mathcal{C}_T(\mathcal{P}) := \mathop{\mathbb{E}}_{\mathcal{T} \sim P^T} \mathop{\mathbb{E}}_{\boldsymbol{\sigma}} \left[ \sup_{\{\Pi_c\} \in \mathcal{P}} \sum_c \mathrm{Tr}[\Pi_c Q_{c,\boldsymbol{\sigma}}^{\mathcal{T}}] \right] \ . \tag{A11}$$

In the following sections we show how to bound $\mathcal{C}_T(\mathcal{P})$ using quantities that can be easily computed for a given embedding $x \mapsto \rho(x)$. The main technical result that allows such simple expressions is the following

**Lemma 1.** *Let $A_i$ be a set of operators and $i$ a random variable with probability distribution $p_i$. Then*

$$\mathop{\mathbb{E}}_{i \sim p} (\|A_i\|_1) \leq \mathrm{Tr} \sqrt{\mathop{\mathbb{E}}_{i \sim p} \left( A_i A_i^{\dagger} \right)} \ , \tag{A12}$$

*where $\mathbb{E}_{i \sim p} f(i) := \sum_i p_i f(i)$.*

*Proof:* We define the positive operators $X_i := \sqrt{A_i A_i^{\dagger}}$. Thanks to the definition of trace norm $\|A\|_1 = \mathrm{Tr} \sqrt{AA^{\dagger}}$ and the linearity of the trace, it is sufficient to prove that

$$\sum_i p_i X_i \leq \sqrt{\sum_i p_i X_i^2} \ , \tag{A13}$$

where the operator inequality $Y \geq 0$ means that $Y$ is a positive operator. The above inequality is proven as follows. Since the function $f(x) = x^2$ is operator convex [45], we may write

$$\left(\sum_i p_i X_i\right)^2 \leq \sum_i p_i X_i^2 . \qquad (A14)$$

Moreover, since $g(x) = \sqrt{x}$ is operator monotone [45] we may take the square root of both sides of the above equation and get (A13). Note that a convex combination of positive matrices is also positive, so the left hand side of (A13) is a positive operator, and thus is equal to the square root of its square. This completes the proof. $\square$

We are now ready to write the main result of this section, namely a bound that allows us to express the Rademacher complexity of the quantum classifier via the quantity that was introduced in (10). We focus on binary classification problems, where there are two possible classes, which we call 0 and 1, so $c \in \{0, 1\}$ and a POVM consists of two positive operators, $\Pi_0$ and $\Pi_1 = 1 - \Pi_0$. Then, we extend the result to a general multiary classification problem with $N_C$ classes.

**Theorem 1.** *For binary classification problems with fixed embedding $x \mapsto \rho(x)$ and POVM $\mathcal{P}_2 = \{\Pi, 1 - \Pi\}$, we find*

$$\mathcal{C}_T(\mathcal{P}_2) \leq \frac{1}{2\sqrt{T}} \operatorname{Tr} \sqrt{\sum_x P(x)\rho(x)^2} = \frac{1}{2}\sqrt{\frac{\mathcal{B}}{T}}, \quad (A15)$$

*where $\mathcal{B}$ was defined in Eq. (10). For multiary classification problems with $N$ classes we get*

$$\mathcal{C}_T(\mathcal{P}_{N_C}) \leq \sqrt{\frac{N_C \mathcal{B}}{T}}, \qquad (A16)$$

*which is slightly larger than (A15) when $N_C = 2$.*

*Proof:* We first focus on binary classification problems. Since constant terms are averaged out we can write Eq. (A11), for $\Pi_0 = \Pi$ and $\Pi_1 = 1 - \Pi$, as

$$\mathcal{C}_T(\mathcal{P}_2) = \underset{\mathcal{T} \sim P^T}{\mathbb{E}} \underset{\boldsymbol{\sigma}}{\mathbb{E}} \left[\sup_{\Pi} \operatorname{Tr}[\Pi(Q_{0,\boldsymbol{\sigma}}^{\mathcal{T}} - Q_{1,\boldsymbol{\sigma}}^{\mathcal{T}})]\right] , \quad (A17)$$

where again the constant term is averaged out. The maximization over $\Pi$ can be done by adapting the Helstrom theorem (see Theorem 13.2 in [46]):

$$\underset{\boldsymbol{\sigma}}{\mathbb{E}} \left[\sup_{\Pi} \operatorname{Tr}[\Pi(Q_{0,\boldsymbol{\sigma}}^{\mathcal{T}} - Q_{1,\boldsymbol{\sigma}}^{\mathcal{T}})]\right] \leq$$

$$\frac{1}{2}\underset{\boldsymbol{\sigma}}{\mathbb{E}} \sup_{\Pi} \left[|\operatorname{Tr}[\Pi_0(Q_{0,\boldsymbol{\sigma}}^{\mathcal{T}} - Q_{1,\boldsymbol{\sigma}}^{\mathcal{T}})]| + |\operatorname{Tr}[\Pi_1(Q_{0,\boldsymbol{\sigma}}^{\mathcal{T}} - Q_{1,\boldsymbol{\sigma}}^{\mathcal{T}})]|\right] \leq$$

$$\frac{1}{2}\underset{\boldsymbol{\sigma}}{\mathbb{E}} \sup_{\Pi} \left[\operatorname{Tr}[\Pi_0|Q_{0,\boldsymbol{\sigma}}^{\mathcal{T}} - Q_{1,\boldsymbol{\sigma}}^{\mathcal{T}}|] + \operatorname{Tr}[\Pi_1|Q_{0,\boldsymbol{\sigma}}^{\mathcal{T}} - Q_{1,\boldsymbol{\sigma}}^{\mathcal{T}}|]\right] \leq$$

$$\frac{1}{2}\underset{\boldsymbol{\sigma}}{\mathbb{E}} \operatorname{Tr}[|Q_{0,\boldsymbol{\sigma}}^{\mathcal{T}} - Q_{1,\boldsymbol{\sigma}}^{\mathcal{T}}|],$$

where $|A| = \sqrt{AA^\dagger}$ and $\|A\|_1 = \operatorname{Tr}|A|$. In the first inequality, we are again able to average out the constant term, despite the fact it is within an absolute difference, because setting $\boldsymbol{\sigma} \to -\boldsymbol{\sigma}$ changes its sign whilst not affecting the other term in the absolute difference. The second inequality comes from the fact that $|\operatorname{Tr}[AB]| \leq \operatorname{Tr}[A|B|]$ for any operator B and positive operator A. The third inequality comes from the linearity of the trace and the fact that the elements of the POVM sum to the identity. Therefore,

$$\mathcal{C}_T(\mathcal{P}_2) \leq \underset{\mathcal{T} \sim P^T}{\mathbb{E}} \underset{\boldsymbol{\sigma}}{\mathbb{E}} \left[\frac{\|Q_{0,\boldsymbol{\sigma}}^{\mathcal{T}} - Q_{1,\boldsymbol{\sigma}}^{\mathcal{T}}\|_1}{2}\right] \qquad (A18)$$

$$= \underset{\mathcal{T} \sim P^T}{\mathbb{E}} \underset{\boldsymbol{\sigma}}{\mathbb{E}} \left\|\frac{1}{2T}\sum_{k=1}^T (\delta_{c_k,0} - \delta_{c_k,1})\sigma_k\rho(x_k)\right\|_1 .$$

An alternative proof of the above inequality without the $1/2$, is by using the definition [35] of the trace norm $\|A\|_1 = \max_{B:\|B\|_\infty \leq 1} \operatorname{Tr}[AB]$, and noting that $\|\Pi\|_\infty \leq 1$ for elements of the POVM. We now use Eq. (A12) to get

$$\mathcal{C}_T(\mathcal{P}_2) \leq \frac{1}{2} \operatorname{Tr} \sqrt{\underset{\mathcal{T} \sim P^T}{\mathbb{E}} \underset{\boldsymbol{\sigma}}{\mathbb{E}} \left(Q_{0,\boldsymbol{\sigma}}^{\mathcal{T}} - Q_{1,\boldsymbol{\sigma}}^{\mathcal{T}}\right)^2} , \qquad (A19)$$

and by explicit calculation

$$\left(Q_{0,\boldsymbol{\sigma}}^{\mathcal{T}} - Q_{1,\boldsymbol{\sigma}}^{\mathcal{T}}\right)^2 = \frac{1}{T^2} \sum_{k,j=1}^T (\delta_{c_k,0} - \delta_{c_k,1})(\delta_{c_j,0} - \delta_{c_j,1})\times$$

$$\sigma_k\sigma_j\rho(x_k)\rho(x_j). \qquad (A20)$$

Since the $\sigma_j$s are independent and with zero mean, we get

$$\underset{\mathcal{T} \sim P^T}{\mathbb{E}} \underset{\boldsymbol{\sigma}}{\mathbb{E}} \left(Q_{0,\boldsymbol{\sigma}}^{\mathcal{T}} - Q_{1,\boldsymbol{\sigma}}^{\mathcal{T}}\right)^2 = \underset{\mathcal{T} \sim P^T}{\mathbb{E}} \sum_{k=1}^T \frac{(\delta_{c_k,0} - \delta_{c_k,1})^2}{T^2}\rho(x_k)^2$$

$$= \underset{(c,x) \sim P}{\mathbb{E}} \left[\frac{1}{T}\rho(x)^2\right] , \qquad (A21)$$

where we used the fact that $(\delta_{c_k,0} - \delta_{c_k,1})^2 = 1$ and that $(c_k, x_k)$ are independent and identically distributed. Inserting the above equation into (A19) and using $P(x) = \sum_c P(c,x)$ we get (A15), which completes the first part of the theorem.

For the multiary classification problem with $N_C$ equiprobable classes, using Hölder's inequality in (A11),

and noting that $\|\Pi_c\|_\infty \leq 1$, we may write

$$\mathcal{C}_T(\mathcal{P}_{N_C}) \leq \underset{\mathcal{T} \sim P^T}{\mathbb{E}} \underset{\boldsymbol{\sigma}}{\mathbb{E}} \sum_c \|Q_{c,\boldsymbol{\sigma}}^{\mathcal{T}}\|_1 \qquad (A22)$$

$$\leq N_C \underset{\mathcal{T} \sim P^T}{\mathbb{E}} \underset{\boldsymbol{\sigma}}{\mathbb{E}} \underset{c}{\mathbb{E}} \|Q_{c,\boldsymbol{\sigma}}^{\mathcal{T}}\|_1 \qquad (A23)$$

$$\leq N_C \operatorname{Tr} \sqrt{\underset{\mathcal{T} \sim P^T}{\mathbb{E}} \underset{\boldsymbol{\sigma}}{\mathbb{E}} \underset{c}{\mathbb{E}} (Q_{c,\boldsymbol{\sigma}}^{\mathcal{T}})^2} \qquad (A24)$$

$$\leq N_C \operatorname{Tr} \sqrt{\frac{1}{N_C T} \sum_{c,x} P(c,x)\rho(x)^2} \qquad (A25)$$

$$\leq \sqrt{\frac{N_C}{T}} \operatorname{Tr} \sqrt{\sum_x P(x)\rho(x)^2}, \qquad (A26)$$

where in the second line we have substituted the sum over $c$ with an average where $c$ is sampled from the uniform distribution with $p_c = 1/N_C$, in the third line we use Eq. (A12), in the fourth line we perform the averages as in Eq. (A21), and in the last line we simply employ the marginal distribution, as in Eq. (A15). $\qquad \square$

### 3. Bound on the approximation error

In this section we focus on the approximation error (14) and prove the following important result.

**Theorem 2.** *Given some $x$-dependent states $\rho(x)$, if we define an embedding using $N$ copies $x \mapsto \rho(x)^{\otimes N}$, then $\mathcal{A} \to 0$ for $N \to \infty$ as long as $F(\rho(x), \rho(y)) \neq 0$ for $x \neq y$. Moreover,*

$$\lim_{N \to \infty} \frac{\log \mathcal{A}}{N} \leq \log F_{\max} \qquad (A27)$$

*where $F_{\max} = \max_{x \neq y} F(\rho(x), \rho(y))$.*

*Proof:* From the definition of the approximation error $\mathcal{A} = R(h^*) - R^{\text{Bayes}}$, we write

$$R = \sum_x \sum_{c \neq c'} P(c,x) \operatorname{Tr}[\Pi_{c'}^* \rho(x)], \qquad (A28)$$

$$R^{\text{Bayes}} = \sum_x \sum_{c \neq c'} P(c,x)\ell^{\text{Bayes}}(c',x), \qquad (A29)$$

where $\ell^{\text{Bayes}}(c,x) = \delta_{c,b(x)}$ and $b(x) = \operatorname{argmax}_c P(c|x)$. Note that the second summation is over all $c$ and $c'$ such that $c \neq c'$. Therefore,

$$\mathcal{A} = \sum_x \sum_{c \neq c'} P(x,c) \left( \operatorname{Tr}[\Pi_{c'}^* \rho(x)] - \delta_{c',b(x)} \right) \qquad (A30)$$

The approximation error is calculated using the optimal measurement for a given encoding $\rho(x)$, however we can upper bound it by replacing this optimal measurement with a suboptimal measurement. We may find a sub-optimal strategy as follows: we know that there always exists some POVM $\Pi_x$ that obeys [10, 47]

$$q(x) \operatorname{Tr}[\Pi_y \rho(x)] \leq \sqrt{q(x)q(y)} F(\rho(x), \rho(y)), \qquad (A31)$$

for any probability distribution $q(x)$. From $\Pi_x$ we can then construct the POVM $\Pi_c$ as follows

$$\Pi_c = \sum_x \delta_{c,b(x)} \Pi_x, \qquad (A32)$$

namely we first try to learn the value of $x$, and then perform the standard Bayesian classification to get the class. Now there are many possibilities to find bounds depending on the choice of $q(x)$ in (A31). Here we chose to use $q(x) = p(x|c)$, namely we train the measurements to recognise all inputs within a certain class, and then check whether the Bayes classifier predicts a different result. We may write

$$\mathcal{A} \leq \sum_x \sum_{c \neq c'} P(c)P(x|c) \left[ \sum_y \delta_{c',b(y)} \operatorname{Tr}[\Pi_y \rho(x)] - \delta_{c',b(x)} \right]$$

$$= \sum_x \sum_{c \neq c'} P(c) \left[ \sum_y \delta_{c',b(y)} \mathcal{F}_{xy}^c - P(x|c)\delta_{c',b(x)} \right]$$

$$= \sum_{x \neq y} \sum_{c \neq b(y)} P(c)\mathcal{F}_{xy}^c, \qquad (A33)$$

where, in the last line, the summation is over all $x$ and $y$ such that $x \neq y$, and where

$$F_{xy}^c = \sqrt{P(x|c)P(y|c)} F(\rho(x), \rho(y)). \qquad (A34)$$

The upper bound (A33) is typically too large to be practical. However, it can be used to show an important result. If we define an embedding as $x \mapsto \rho(x)^{\otimes N}$, then $F_{xy}^c = \sqrt{P(x|c)P(y|c)} F(\rho(x), \rho(y))^N \to 0$ for $N \to \infty$ as long as $F(\rho(x), \rho(y)) \neq 0$. Moreover, since $F(\rho(x), \rho(y)) \leq F_{\max}$, we get Eq. (A27). $\qquad \square$

Thanks to the above theorem, we see that taking copies of a simple embedding guarantees that $\mathcal{A} \to 0$ for $N \to \infty$, as we observe in the numerical simulations shown in Fig. 4.

### 4. Further inequalities

In this section we discuss other inequalities and connections with other entropic quantities. We first recall the following inequality, which will be extensively used in this section:

$$\operatorname{Tr} \sqrt{\sum_i X_i} \leq \sum_i \operatorname{Tr} \sqrt{X_i}, \qquad (A35)$$

which is valid for any set of positive operators $X_i$ (see Ref. [48] for a proof).

We first discuss the risk (1) and empirical risk (2) for multiary classification problems with $N_C$ classes. In this case there is no known analytic form of the optimal POVM, but suboptimal choices can be constructed using

pretty good measurements [10, 49]: calling $T_c$ the number of samples in the training set with class $c$, we may write $R_{\mathcal{T}}(\Pi) = 1 - \sum_c \frac{T_c}{T} \text{Tr}[\Pi_c \rho_c^{\mathcal{T}}]$ and the error for an optimal measurement can be bounded as [10, 49]

$$R_{\mathcal{T}}(\Pi^{\mathcal{T}}) \leq \sum_{c \neq c'} \frac{\sqrt{T_c T_{c'}}}{T} F(\rho_c^{\mathcal{T}}, \rho_{c'}^{\mathcal{T}}), \qquad (A36)$$

where $F(\rho, \sigma) = \|\sqrt{\rho}\sqrt{\sigma}\|_1$ is the quantum fidelity. Using the strong concavity of the fidelity

$$\mathbb{E}_{\mathcal{T}} R_{\mathcal{T}}(\Pi^{\mathcal{T}}) \leq \sum_{c \neq c'} \frac{\sqrt{T_c T_{c'}}}{T} F(\rho_c, \rho_{c'}), \qquad (A37)$$

which is a multiclass generalization of (18). Therefore, even for classification problems with $N_C > 2$ low risk is possible when the fidelity between the average states with inputs belonging to different classes is low.

As for the generalization error, we see that the complexity $\mathcal{B}$ defined in Eq. (10) does not depend on the classes. Nonetheless, using (A35) we also get the following inequalities

$$\mathcal{B} \leq \left( \sum_c \sqrt{P(c)\mathcal{B}_c} \right)^2, \qquad (A38)$$

$$\mathcal{B}_c = \left( \text{Tr} \sqrt{\sum_x P(x|c)\rho(x)^2} \right)^2. \qquad (A39)$$

Setting $\sigma_c = \sum_x P(x|c)\rho(x)^2 = \sum_{i=1}^{r_c} \lambda_i |\lambda_i\rangle\langle\lambda_i|$, where $r_c$ is the rank of $\sigma_c$, we find

$$\mathcal{B}_c = \left( \sum_i \sqrt{\lambda_i} \right)^2 = \sum_i \lambda_i + \sum_{i \neq j} \sqrt{\lambda_i \lambda_j}. \qquad (A40)$$

Thanks to Jensen's inequality, for every set of positive $x_i$ of size $n$, we can write $\sum_{i=1}^n \sqrt{x_i} \leq \sqrt{n \sum_{i=1}^n x_i}$. In Eq. (A40), the number of terms in the second sum is $r_c^2 - r_c$, so

$$\mathcal{B}_c \leq \sum_i \lambda_i + \sqrt{(r_c^2 - r_c) \sum_{i \neq j} \lambda_i \lambda_j} \qquad (A41)$$

$$= \sum_i \lambda_i + \sqrt{(r_c^2 - r_c) \left( \sum_{i,j} \lambda_i \lambda_j - \sum_i \lambda_i^2 \right)} \qquad (A42)$$

$$= \text{Tr}[\sigma_c] + \sqrt{(r_c^2 - r_c)(\text{Tr}[\sigma_c]^2 - \text{Tr}[\sigma_c^2])}. \qquad (A43)$$

For pure state embeddings, $\sigma_c = \rho_c$ and we get (19).

Another interesting bound can be found by applying the Cauchy-Schwarz inequality $\text{Tr}[\sqrt{X}]^2 \leq \text{Tr}[X]\text{Tr}[\mathbb{1}]$ to (10). We find

$$\mathcal{B} \leq D \sum_x P(x) \text{Tr}[\rho(x)^2] \leq D, \qquad (A44)$$

where $D$ is the dimension of the embedding Hilbert space.

We now study the embedding $\rho(x)$ using tools from quantum information. We define an extended tripartite mixed $\rho_{CXQ}$ state as in Eq. (11), where $CX$ is the data Hilbert space, $C$ is spanned by the classes $|c\rangle$ and $X$ by the labels $|x\rangle$, while $Q$ is the Hilbert space of the quantum embedding $\rho(x)$. We now introduce the Rényi conditional mutual information of $\rho_{CXQ}$ following Prop. 8 from [31]

$$I_\alpha(X{:}Q|C) = \qquad (A45)$$
$$\frac{\alpha}{\alpha - 1} \log_2 \text{Tr} \left( \left[ \rho_C^{\frac{\alpha-1}{2}} \underset{X}{\text{Tr}} \left( \rho_{CX}^{\frac{1-\alpha}{2}} \rho_{CXQ}^\alpha \rho_{CX}^{\frac{1-\alpha}{2}} \right) \rho_C^{\frac{\alpha-1}{2}} \right]^{\frac{1}{\alpha}} \right),$$

where $\rho_{CX} = \text{Tr}_Q[\rho_{CXQ}] = \sum_{xc} P(c,x)|cx\rangle\langle cx|$, and $\rho_C = \text{Tr}_X[\rho_{XC}] = \sum_c P(c)|c\rangle\langle c|$. When multiplying operators that span different Hilbert spaces, it is implicit that the operators take a tensor product with the identity on the spaces that they do not span (e.g., $\rho_{CX}\rho_{CXQ} = (\rho_{CX} \otimes \mathbb{1}_Q)\rho_{CXQ}$). By explicit computation

$$\underset{X}{\text{Tr}} \left( \rho_{CX}^{\frac{1-\alpha}{2}} \rho_{CXQ}^\alpha \rho_{CX}^{\frac{1-\alpha}{2}} \right) = \qquad (A46)$$
$$\sum_{cx} P(c,x)^{1-\alpha} P(c,x)^\alpha |c\rangle\langle c| \otimes \rho(x)^\alpha =$$
$$\sum_{cx} P(c,x)|c\rangle\langle c| \otimes \rho(x)^\alpha,$$

$$\rho_C^{\frac{\alpha-1}{2}} \underset{X}{\text{Tr}} \left( \rho_{CX}^{\frac{1-\alpha}{2}} \rho_{CXQ}^\alpha \rho_{CX}^{\frac{1-\alpha}{2}} \right) \rho_C^{\frac{\alpha-1}{2}} = \qquad (A47)$$
$$\sum_{cx} P(c,x)P(c)^{\alpha-1}|c\rangle\langle c| \otimes \rho(x)^\alpha =$$
$$\sum_{cx} P(x|c)P(c)^\alpha |c\rangle\langle c| \otimes \rho(x)^\alpha$$

and

$$I_\alpha(X{:}Q|C) = \qquad (A48)$$
$$\frac{\alpha}{\alpha - 1} \log_2 \left[ \sum_c P(c) \text{Tr} \left( \left[ \sum_x P(x|c)\rho(x)^\alpha \right]^{\frac{1}{\alpha}} \right) \right].$$

We note a similarity between the above expression and the quantities that are found in the generalization bound (A39). Indeed, for a uniform distribution over $N_C$ classes, $P(c) = 1/N_C$, i.e., when all classes are equally likely, we find from (A39) that

$$\mathcal{B} \leq 2^{I_2(X{:}Q|C)} N_C, \qquad (A49)$$

and thus show a direct link between the generalization bound and the Rényi conditional mutual information of $\rho_{CXQ}$. Therefore, good generalization is possible whenever $I_2(X{:}Q|C)$ is small or for large training sets $T \gg 2^{I_2(X{:}Q|C)} N_C$.

We can interpret the space $Q$ in (11) as compression of the input into a quantum state. Assuming that the conclusions from Ref. [41] (which were originally formulated

for the classical Shannon entropy) can be trivially extended to Rényi entropies, optimal compression happens when

$$I_\alpha(X{:}Q|C) = I_\alpha(X{:}C|Q) = I_\alpha(C{:}Q|X) = 0. \quad (A50)$$

A zero conditional mutual information means that the three systems form a Markov chain: conditioning over one of the three systems makes the other two mutually independent. Quantum mechanically $I(X{:}Q|C) = 0$ if $\rho_{XQC} = \rho_{XC}^{1/2}\rho_C^{-1/2}\rho_{QC}\rho_C^{-1/2}\rho_{XC}^{1/2}$ [31], which is not generally satisfied by the state (11). According to Ref. [41], we should both minimize $I(X{:}Q|C)$ and maximize $I(C{:}Q)$. The Rényi generalization of $I(C{:}Q)$ can be obtained using a similar expression to (A45), by applying the expression for conditional mutual information to a state that is independent of the conditioning system (i.e., by calculating $I(C{:}Q|X)$ for the state $\rho_{CQ} \otimes \rho_X$). We get the expression

$$I_\alpha(C{:}Q) = \frac{\alpha}{\alpha-1} \log_2 \mathrm{Tr}\left( \left[ \mathop{\mathrm{Tr}}_C \left( \rho_C^{\frac{1-\alpha}{2}} \rho_{CQ}^\alpha \rho_C^{\frac{1-\alpha}{2}} \right) \right]^{\frac{1}{\alpha}} \right)$$
$$= \frac{\alpha}{\alpha-1} \log_2 \mathrm{Tr}\left( \left[ \sum_c P(c)\rho_c^\alpha \right]^{\frac{1}{\alpha}} \right), \quad (A51)$$

where $\rho_c$ was introduced in Eq. (5). Simpler expressions that are directly connected with the fidelity may be obtained when for $\alpha = 1/2$. For pure state embeddings $\rho(x)^\alpha = \rho(x)$ and we get

$$I_{1/2}(X{:}Q|C) = -\log_2 \sum_c P(c)\,\mathrm{Tr}\left( \left[ \sum_x P(x|c)\sqrt{\rho(x)} \right]^2 \right)$$
$$= -\log_2 \sum_c P(c)\mathcal{F}(c), \quad (A52)$$

where

$$\mathcal{F}(c) = \sum_{x,y} P(x|c)P(y|c)F(\rho(x),\rho(y))^2, \quad (A53)$$

is the average squared fidelity between embeddings of inputs from the same class $c$. Therefore, $\mathcal{F}(c)$ should be maximized to minimize $I_{1/2}(X{:}Q|C)$. In other words, low conditional mutual information is possible when $F(\rho(x),\rho(y)) \simeq 1$ for $x$ and $y$ belonging to the same class. Moreover,

$$-I_{1/2}(C{:}Q) = \log_2 \mathrm{Tr}\left[ \sum_c P(c)\sqrt{\rho_c} \right]^2 \quad (A54)$$
$$= \log_2 \left[ \sum_c P(c)^2 + \sum_{c\neq c'} P(c)P(c')\mathcal{F}(c,c') \right],$$

where

$$\mathcal{F}(c,c') = \mathrm{Tr}[\sqrt{\rho_c}\sqrt{\rho_{c'}}] \leq F(\rho_c,\rho_{c'}) \quad (A55)$$

is related to the fidelity between the average states $\rho_c$ and $\rho_{c'}$ for different classes. Since the logarithm is monotonic, the minimization of $-I_{1/2}(C{:}Q)$ is possible by minimizing $F(\rho_c,\rho_{c'})$. Therefore, using Rényi entropies with $\alpha = 1/2$, we recover the same conclusions as in the previous section: *a good embedding is one for which the fidelity between two embedded states is small if the inputs are from different classes and high if the inputs are from the same class.*

---

[1] J. Biamonte, P. Wittek, N. Pancotti, P. Rebentrost, N. Wiebe, and S. Lloyd, Quantum machine learning, Nature **549**, 195 (2017).

[2] M. Schuld, *Supervised learning with quantum computers* (Springer, 2018).

[3] V. Dunjko and H. J. Briegel, Machine learning & artif. intell. in the quantum domain: a review of recent progress, Rep. Prog. Phys. **81**, 074001 (2018).

[4] G. Carleo, I. Cirac, K. Cranmer, L. Daudet, M. Schuld, N. Tishby, L. Vogt-Maranto, and L. Zdeborová, Machine learning and the physical sciences, Reviews of Modern Physics **91**, 045002 (2019).

[5] M. Schuld and N. Killoran, Quantum machine learning in feature hilbert spaces, Physical review letters **122**, 040504 (2019).

[6] V. Havlíček, A. D. Córcoles, K. Temme, A. W. Harrow, A. Kandala, J. M. Chow, and J. M. Gambetta, Supervised learning with quantum-enhanced feature spaces, Nature **567**, 209 (2019).

[7] S. Lloyd, M. Schuld, A. Ijaz, J. Izaac, and N. Killoran, Quantum embeddings for machine learning, arXiv preprint arXiv:2001.03622 (2020).

[8] I. Cong, S. Choi, and M. D. Lukin, Quantum convolutional neural networks, Nature Physics **15**, 1273 (2019).

[9] H.-Y. Huang, M. Broughton, M. Mohseni, R. Babbush, S. Boixo, H. Neven, and J. R. McClean, Power of data in quantum machine learning, arXiv preprint arXiv:2011.01938 (2020).

[10] L. Banchi, Q. Zhuang, and S. Pirandola, Quantum-enhanced barcode decoding and pattern recognition, Physical Review Applied **14**, 064026 (2020).

[11] H.-Y. Huang, R. Kueng, and J. Preskill, Information-theoretic bounds on quantum advantage in machine learning, arXiv preprint arXiv:2101.02464 (2021).

[12] C. Ciliberto, A. Rocchetto, A. Rudi, and L. Wossnig, Fast quantum learning with statistical guarantees, arXiv

preprint arXiv:2001.10477 (2020).

[13] K. Mitarai, M. Negoro, M. Kitagawa, and K. Fujii, Quantum circuit learning, Physical Review A **98**, 032309 (2018).

[14] M. Benedetti, E. Lloyd, S. Sack, and M. Fiorentini, Parameterized quantum circuits as machine learning models, Quantum Science and Technology **4**, 043001 (2019).

[15] J.-G. Liu and L. Wang, Differentiable learning of quantum circuit born machines, Physical Review A **98**, 062324 (2018).

[16] S. Pirandola, B. R. Bardhan, T. Gehring, C. Weedbrook, and S. Lloyd, Advances in photonic quantum sensing, Nature Photon. **12**, 724 (2018).

[17] S. Lloyd, Enhanced sensitivity of photodetection via quantum illumination, Science **321**, 1463 (2008).

[18] S.-H. Tan, B. I. Erkmen, V. Giovannetti, S. Guha, S. Lloyd, L. Maccone, S. Pirandola, and J. H. Shapiro, Quantum illumination with gaussian states, Phys. Rev. Lett. **101**, 253601 (2008).

[19] S. Barzanjeh, S. Guha, C. Weedbrook, D. Vitali, J. H. Shapiro, and S. Pirandola, Microwave quantum illumination, Phys. Rev. Lett. **114**, 080503 (2015).

[20] S. Pirandola, Quantum reading of a classical digital memory, Phys. Rev. Lett. **106**, 090504 (2011).

[21] G. Ortolano, E. Losero, S. Pirandola, M. Genovese, and I. Ruo-Berchera, Experimental quantum reading with photon counting, Science Advances **7**, eabc7796 (2021).

[22] Q. Zhuang and S. Pirandola, Entanglement-enhanced testing of multiple quantum hypotheses, Commun. Phys **3**, 103 (2020).

[23] H. Shi, Z. Zhang, S. Pirandola, and Q. Zhuang, Entanglement-assisted absorption spectroscopy, Phys. Rev. Lett. **125**, 180502 (2020).

[24] H.-C. Cheng, M.-H. Hsieh, and P.-C. Yeh, The learnability of unknown quantum measurements, arXiv preprint arXiv:1501.00559 (2015).

[25] A. Abbas, D. Sutter, C. Zoufal, A. Lucchi, A. Figalli, and S. Woerner, The power of quantum neural networks, arXiv preprint arXiv:2011.00027 (2020).

[26] J. Bae and L.-C. Kwek, Quantum state discrimination and its applications, Journal of Physics A: Mathematical and Theoretical **48**, 083001 (2015).

[27] N. Tishby, F. C. Pereira, and W. Bialek, The information bottleneck method, arXiv preprint physics/0004057 (2000).

[28] C. W. Helstrom and C. W. Helstrom, *Quantum detection and estimation theory*, Vol. 3 (Academic press New York, 1976).

[29] S. Shalev-Shwartz and S. Ben-David, *Understanding machine learning: From theory to algorithms* (Cambridge university press, 2014).

[30] M. Belkin, D. Hsu, S. Ma, and S. Mandal, Reconciling modern machine-learning practice and the classical bias–variance trade-off, Proceedings of the National Academy of Sciences **116**, 15849 (2019).

[31] M. Berta, K. P. Seshadreesan, and M. M. Wilde, Rényi generalizations of the conditional quantum mutual information, Journal of Mathematical Physics **56**, 022205 (2015).

[32] K. M. Audenaert, J. Calsamiglia, R. Munoz-Tapia, E. Bagan, L. Masanes, A. Acin, and F. Verstraete, Discriminating states: The quantum chernoff bound, Physical review letters **98**, 160501 (2007).

[33] R. Konig, R. Renner, and C. Schaffner, The operational meaning of min-and max-entropy, IEEE Transactions on Information theory **55**, 4337 (2009).

[34] M. Tomamichel, R. Colbeck, and R. Renner, A fully quantum asymptotic equipartition property, IEEE Transactions on information theory **55**, 5840 (2009).

[35] J. Watrous, *The theory of quantum information* (Cambridge University Press, 2018).

[36] E. Farhi and H. Neven, Classification with quantum neural networks on near term processors, arXiv preprint arXiv:1802.06002 (2018).

[37] D. Haussler and M. Opper, General bounds on the mutual information between a parameter and n conditionally independent observations, in *Proceedings of the eighth annual conference on Computational learning theory* (1995) pp. 402–411.

[38] D. Haussler and M. Opper, Mutual information and bayes methods for learning a distribution, in *Proc. Workshop on the Theory of Neural Networks: The Statistical Mechanics Perspective. World Scientific* (1995).

[39] S. Oh, J. Choi, and J. Kim, A tutorial on quantum convolutional neural networks (qcnn), in *2020 International Conference on Information and Communication Technology Convergence (ICTC)* (IEEE, 2020) pp. 236–239.

[40] A. Pesah, M. Cerezo, S. Wang, T. Volkoff, A. T. Sornborger, and P. J. Coles, Absence of barren plateaus in quantum convolutional neural networks, arXiv preprint arXiv:2011.02966 (2020).

[41] I. Fischer, The conditional entropy bottleneck, arXiv preprint arXiv:2002.05379 (2020).

[42] S. Salek, D. Cadamuro, P. Kammerlander, and K. Wiesner, Quantum rate-distortion coding of relevant information, IEEE Transactions on Information Theory **65**, 2603 (2018).

[43] N. Datta, C. Hirche, and A. Winter, Convexity and operational interpretation of the quantum information bottleneck function, in *2019 IEEE International Symposium on Information Theory (ISIT)* (IEEE, 2019) pp. 1157–1161.

[44] A. S. Holevo, Bounds for the quantity of information transmitted by a quantum communication channel, Problemy Peredachi Informatsii **9**, 3 (1973).

[45] E. Carlen, Trace inequalities and quantum entropy: an introductory course, Entropy and the quantum **529**, 73 (2010).

[46] I. Bengtsson and K. Życzkowski, *Geometry of quantum states: an introduction to quantum entanglement* (Cambridge university press, 2017).

[47] A. Montanaro, Pretty simple bounds on quantum state discrimination, arXiv preprint arXiv:1908.08312 (2019).

[48] K. M. Audenaert and M. Mosonyi, Upper bounds on the error probabilities and asymptotic error exponents in quantum multiple state discrimination, Journal of Mathematical Physics **55**, 102201 (2014).

[49] H. Barnum and E. Knill, Reversing quantum dynamics with near-optimal quantum and classical fidelity, Journal of Mathematical Physics **43**, 2097 (2002).